Proceedings of the ASME 2021
International Mechanical Engineering Congress and Exposition
IMECE2021
November 1-5, 2021, Virtual Online

IMECE2021-73372

BIPHASIC REPRESENTATIVE ELEMENTAL VOLUMES FOR 3-D WHITE MATTER ELASTOGRAPHY

Xuehai Wu[1], John G. Georgiadis[2], and Assimina A. Pelegri[1]

[1]Rutgers, The State University of New Jersey
Piscataway, NJ, USA

[2]Illinois Institute of Technology
Chicago, IL, USA

ABSTRACT

White matter (WM) characterization is challenging due to its anisotropic and inhomogeneous microstructure that necessitates multiscale and multi-modality measurements. Shear elastography is one such modality that requires the accurate interpretation of 3D shear strain measurements, which hinge on developing appropriate constitutive tissue models. Finite element methods enable the development of such models by simulating the shear response of representative elemental volumes (REV). We have developed triphasic (axon, myelin, glia), 2D REVs to simulate the influence of the intrinsic viscoelastic property and volume fraction of each phase. This work constitutes the extension of 2D- to 3D-REVs, focusing on the effect of the intrinsic material properties and their 3D representation on the viscoelastic response of the tissue. By lumping the axon and myelin phases, a flexible 3D REV generation and analysis routine is then developed to allow for shear homogenization in both the axial and transverse directions. The 2D and 3D models agree on stress distribution and total deformation when 2D cross-sectional snapshots are compared. We also conclude that the ratio of transverse to axial transverse modulus is larger than one when axon fibers are stiffer than the glial phase.

Keywords: white matter, elastography, computational modeling, finite elements, homogenization, viscoelasticity

1. INTRODUCTION

Shear elastography methods based on MRI [1] or ultrasound [2] involve acquiring shear deformation data, followed by solving an inverse problem (based on a tissue constitutive model) to estimate the local mechanical properties, such as stiffness. The interpretation of these voxel-averaged (effective) properties in terms of tissue microarchitecture and intrinsic properties of its constituent cells requires accurate tissue-based models. White matter (WM) is known to be mechanically anisotropic under shear on the millimeter scale, especially in regions with high directional coherence, such as the *corpus callosum* (CC) [3]. By separately exciting the brain in two different directions, the consequences of the mechanical anisotropy of WM have been shown to be very important [4]. While the microstructure anisotropy and diffusional anisotropy are well accepted, the mechanical anisotropy of WM is still debated. Budday et al. [5] concluded that the WM was "not notably anisotropic" at the macroscopic scale after performing mechanical testing ex-vivo on large human WM sections. In an ex-vivo magnetic resonance imaging elastography (MRE) experiments on porcine brain WM blocks surrounding the CC, Schmidt at al. [6] reported that that the axial shear modulus was greater than the transverse, based on a homogeneous inversion model. Lastly, Romano et al. [7] used an orthotropic model to interpret measurements of in-vivo MRE of the human cortical spinal tract (CST). Using a waveguide inversion method that allows to extract a single shear modulus in-vivo for the entire CST WM matter track, they found that the transverse shear stiffness is greater than the axial. Finally, using an inverse transversely isotropic scheme to extract effective shear viscoelastic properties from multi-excitation MRE, Gallo et al. [8] showed that the ratio of transverse to axial stiffness remains greater than 1 in the human CC. Adopting appropriate WM anisotropic models is not only important in brain aging studies [8], but also in traumatic brain injury studies [9].

Our working hypothesis is that WM is anisotropic in shear, and this anisotropy can be related to the intrinsic mechanical properties (of its constituents) and the microstructure. WM consists of a complex network of axon bundles, and each axon in ensheathed in myelin that is produced by glial cells. The disagreement in the WM anisotropy properties reported in the literature can be attributed to differences in experimental methodologies or tissue constitutive models. In order to resolve this issue, we adopt a bottom-up approach: build a micromechanical WM tissue model and then extract the effective properties directly by mimicking the mechanical excitation typical of elastography. One challenge here is to choose the simplest, most economic, model possible to account for those microstructural and mechanical elements that pertain to *our hypothesis*. Rather than starting from an *a priori* constitutive model, we focus here on extending the WM tissue model of Sullivan et al. [10] in 3D. This process is a culmination of prior work [11-15]. The development of the WM tissue model starts by homogenizing representative elemental volumes (REVs) of the microstructure of myelinated brain WM. In [11-12], homogenized REVs (carriers of material properties and geometric information) are assembled to form finite element models based on typical fiber volume fractions calculated by the relative distance between the elements and axonal traces. Our group has also developed another set of WM models that account for discrete axons with tortuous paths and distinct kinematic coupling (ties at random intervals along the axon) [13-14]. Such models recapitulate the distribution of *axon tortuosity* and *myelin coupling* that we discerned from our in-situ characterizations [15].

Seeking to complete the study of the effect of microstructure on WM shear anisotropy, we return to the simplest micromechanical model of WM, which involves a unidirectional composite with axon fibers embedded in a glial matrix. Our prior study [10] involved the mechanics of the transverse plane (perpendicular to the axon direction), so it was only capable of capturing the transverse effective shear moduli. We need to extend the model to 3D in order to explore the response to other shear loading modes. Also, [10] involved a triphasic (axon, myelin, glia) REV, but the sensitivity analysis revealed that the effective moduli of REVs are very sensitive to the fiber volume fraction (which is the sum of the axon and myelin volume fractions), and the intrinsic viscoelastic moduli of the glial phase. It is therefore important to preserve these parameters as we go from 2D to 3D. In the following we perform a systematic study of the harmonic response of a unidirectional composite REV loaded in the transverse and axial plane (parallel to the axon direction). There is no published computational study (to our knowledge) of such models under harmonic shear. Arbogast and Margulies [16] employed approximate expressions for the transverse moduli, while Abolfathi et al. [17] studied viscoelastic relaxation. To our knowledge, the tissue model presented here is used for the first time to model elastography-relevant harmonic shear stress on the cell level.

2. MATERIALS AND METHODS

2.1. Homogenization of axon and myelin composite

The three-dimensional model was generated by extruding a two-dimensional representation of brain white matter consisting of regular hexagonal array of parallel axons with a uniform myelin sheath (**Figure 1**). The two-dimensional REV includes three phases, axon (green), myelin (red), and glial matrix (gray). Using volume fractions of each phase that mimic realistic values for the brain, the sensitivity analysis reported in [10] revealed that the glial matrix properties have the strongest effect on the effective shear response of the material contained in the REV. Therefore, we opt for lumping the two phases (axon and myelin) into one phase, *hereafter renamed "axon"* for simplicity, and maintaining the geometry of the glial matrix. The new 3D REV of the resulting composite (homogenized) biphasic model is depicted in **Figure 1.**

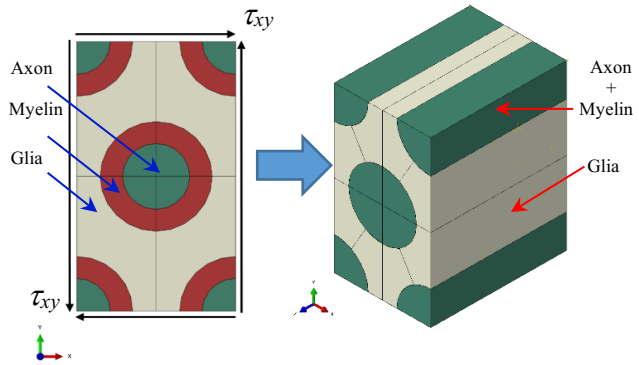

FIGURE 1. *(Left)* 2D triphasic REV under pure shear. The glia, axon, and myelin phases are represented by gray, green and red, respectively. *(Right)* 3D biphasic model, with axon and glia phases, while the geometry and the volume fraction of the glial matrix is maintained.

The creation of the 3D REV (**Figure 2**) allows for deriving effective viscoelastic properties in the axial and transverse directions.

2.2. Finite element analysis and constitutive relationship of REV

An automatic process based on ABAQUS and Python scripting was employed to homogenize the results of the finite element calculations. Harmonic shear loading is applied by imposing shear displacement on exterior opposing boundaries, similar to the 2D REV [10]. A direct steady-state solver was used to solve the equations of motion in the frequency domain. The oscillation frequency of interest is 50 Hz, as this is a common frequency in use for MRE [1]. The constitutive relationship of REVs can be expressed as:

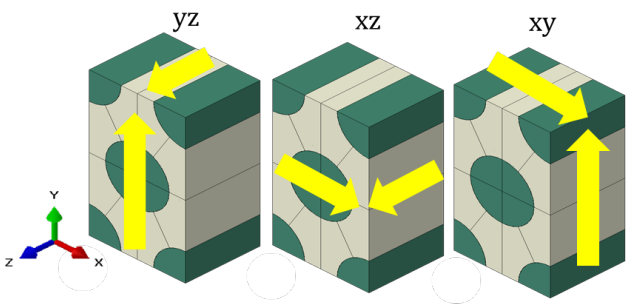

FIGURE 2. Homogenization of axon and myelin composite from 2D triphasic to 3D biphasic REVs. Yellow arrows show shear load in transverse (*xy*) and axial (*yz* and *xz*) directions.

$$\sigma = \left(E'_{eff}(VF) + iE''_{eff}(VF)\right)\varepsilon \tag{1}$$

$$\tau = \left(G'_{eff}(VF) + iG''_{eff}(VF)\right)\gamma \tag{2}$$

$$VF = \frac{\text{Volume of Axon+Myelin}}{\text{Volume of REV}} = \frac{\text{Volume of Lumped Fiber}}{\text{Volume of REV}} \tag{3}$$

where the $\left(E'_{eff}, G'_{eff}\right)$ and $\left(E''_{eff}, G''_{eff}\right)$ are the effective normal/shear storage modulus and normal/shear loss modulus of the tissue REV. (ε, γ) and (σ, υ) are normal/shear strain and normal/shear stress applied on the REV. Each homogenized REV is associated with a particular fiber volume fraction (*VF*). The complete list of intrinsic material properties of axon and glia is: G'_{axon}, G'_{glia}, G''_{axon}, G''_{glia}. The effective moduli, which are functions of *VF* and intrinsic material properties, will be calculated by finite element analysis.

3. EXPERIMENTS AND RESULTS

3.1. Comparing analysis with 2D REV and 3D REV

The 2D REV is meshed with 4-node bilinear, reduced integration elements, which requires approximately 800 finite elements. The 3D REV is meshed with 8-node biquadratic, reduced integration, hybrid elements, which requires approximately 28000 finite elements [18]. A direct steady-state dynamic solver is used to simulate the REV response under a steady harmonic load of 50 Hz. The load is applied as a displacement boundary condition on the surface nodes, with a harmonic displacement parallel to the face of the REV. This boundary condition results in a pure shear deformation of the REV, with a shear strain of γ=0.01 [10] in the axial plane (*xy*-plane) of the 2D and 3D REVs. To reflect the two- and three-dimensionality of the respective REV interfaces, we consider distinct boundary conditions. In the 2D REV, there are three phases axon, myelin, and glia with different geometric interfaces. Considering the lack of literature data on myelin properties, the same values are considered for axon and myelin, with definite boundaries set between them in the computational model. The myelin and glia elements (4-node bilinear elements) share the same nodes. In the 3D REV, the axon and the myelin become a single phase, so there is no interface between them. The 3D axon/glia interface extends to the entire length of the axon. Depending on the contact conditions between the axon and the glia, there may be different tied elements, at regular or random intervals, to represent the nodes of Ranvier. Here, we assume a fully stitched 3D axon/glia interface. Thus, the elements (8-node biquadratic hybrid elements) are fully tied, which means that no interfacial slip is allowed along the length of the axons.

The finite element analysis produces a steady-state harmonic field where the resulting average complex shear stress is computed from the reaction forces. These forces are computed and summed for each phase (glial or axon). As **Equation 2** indicates, the effective shear modulus over the REV is computed by the pure shear stress loading divided by the average shear strain [10].

The intrinsic material properties for both 2D and 3D calculations are $G'_{axon} = 2.15kPa$ (storage modulus), $G''_{axon} = 1.75kPa$ (loss modulus), $G'_{glia} = 0.85kPa$(storage modulus), and $G''_{glia} = 0.3kPa$(loss modulus) [10-11]. The Poisson ratio is assumed $\nu = 0.49$, which is consistent with the white matter incompressibility assumption.

The finite element analysis results of the 2D and 3D REVs illustrate similar global stress distribution (**Figure 3**). There is a slight differentiation between the two models at the 2D axon/myelin/glia or the 3D axon/glia interface. In the 3D REV model, the tie constrain results in a distinct interfacial reaction between the two phases which is more subtle in the 2D REV (common node) model. In spite of the local interface difference, the global stress minima and maxima are concentrated on the same areas within the two REV models. This result supports the consistency of 2D and 3D REV models' behavior in the axial (*xy*-plane) direction. The difference in sub-region around the axon/glia interface indicates the 3D REV sensitivity to the contact information between axon and glia mater.

3.2. 3D REV sensitivity analysis

The purpose of the sensitivity analysis is to systematically study the effect of intrinsic properties (G'_{axon}, G'_{glia}, G''_{axon}, G''_{glia}) on the effective REV properties $\left(G'_{eff}, G''_{eff}\right)$. A total of six variables are defined here, which are derived from a combination of the intrinsic material parameters and the effective properties of REV: $G'_{eff(yz)}/G'_{glia}$, $G'_{eff(xz)}/G'_{glia}$, $G'_{eff(xy)}/G'_{glia}$, $G''_{eff(yz)}/G'_{glia}$, $G''_{eff(xz)}/G'_{glia}$, $G''_{eff(xy)}/G'_{glia}$, where the '*xy*', '*yz*', and '*xz*' are the associated shear moduli's directions.

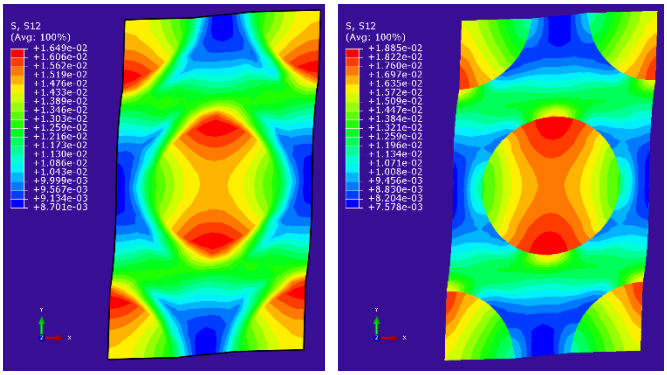

(a) (b)

FIGURE 3. Shear stress distribution for (a) 2D REV and (b) 3D REV in transverse (*xy*-plane) direction. The local stress distribution is smoother in the 2D axon/glia interface where the REV is triphasic the elements share the same 4-nodes, contrasting the 3D case of the tied 8-node lumped fiber with 8-node glial elements. The global shear stress distribution is similar for both cases.

Results are plotted in **Figure 4**, where a logarithmic scale is used for the G'_{axon}/G'_{glia} and G''_{axon}/G''_{glia} axes (ranging from 1 to 100). Note that the independent variables G'_{axon}/G'_{glia} and G''_{axon}/G''_{glia} use the same axis. The range starts from 1 to reflect the fact that the axons are stiffer than the glia [15]. The *VF* of REV is kept at 0.7. The influence of each independent variable on the resulting effective moduli of REV is studied.

Under the correspondence principle, there exist exact solutions for the effective axial moduli, $G'^{*}_{eff(axial)}$ and $G''^{*}_{eff(axial)}$, of unidirectional composites [19]:

$$G'^{*}_{eff(axial)} = G'_{glia}\frac{G'_{axon}(1+VF)+G'_{glia}(1-VF)}{G'_{axon}(1-VF)+G'_{glia}(1+VF)} \quad (4)$$

$$G''^{*}_{eff(axial)} = G''_{glia}\frac{G''_{axon}(1+VF)+G''_{glia}(1-VF)}{G''_{axon}(1-VF)+G''_{glia}(1+VF)} \quad (5)$$

The effective shear moduli in the transverse direction ($G'_{eff(xy)}/G'_{glia}$ and $G''_{eff(xy)}/G'_{glia}$) increase monotonically and are more sensitive to G'_{axon}/G'_{glia} and G''_{axon}/G''_{glia} relative to the axial ones. Note the logarithmic scale in the abscissa. When the axon is stiffer than the glial matrix, the effective transverse shear moduli are larger than the axial. The effective shear moduli ratios pairs in the axial direction match: $G'_{eff(yz)}/G'_{glia} = G'_{eff(xz)}/G'_{glia}$ and $G''_{eff(yz)}/G''_{glia} = G''_{eff(xz)}/G''_{glia}$ which is expected due to the symmetries in the REV. The computed values of $G'^{*}_{eff(axial)}/G'_{glia}$ and $G''^{*}_{eff(axial)}/G'_{glia}$ match with the exact solutions shown in **Equations (4-5)**.

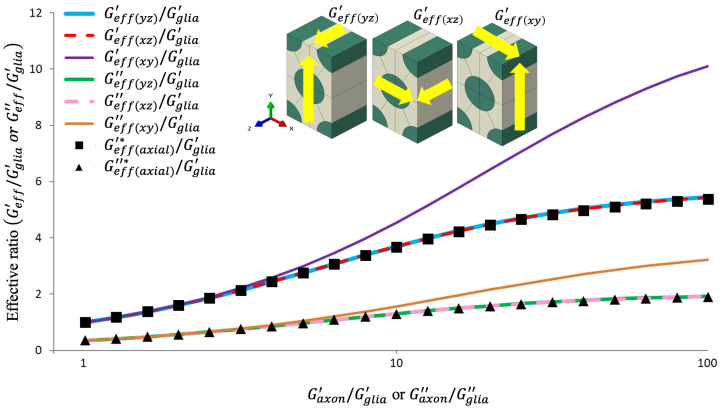

FIGURE 4. Sensitivity analysis of effective properties of the 3D REV for *VF*=0.7. The yellow arrows in the REVs represent the three shear loading directions. $G'^{*}_{eff(axial)}$, $G''^{*}_{eff(axial)}$ denote effective moduli of unidirectional composites. [19] (Although G'_{eff} is noted for the inset the same applies for G''_{eff}.)

In closing, we have to make the following cautionary remark. Under the assumptions made in this paper (isotropic homogeneous and linear viscoelastic constituent materials, perfectly bonded interfaces), the 2D REV model [10] combined with the **Equations [4-5]** are sufficient to estimate all the effective shear moduli of a periodic unidirectional composite. The last conclusion is not self-evident if any of the assumptions are violated, and this justifies the utility of 3D REV models.

4. CONCLUSIONS

Shear elastography methods require the interpretation of the shear deformation data in order to extract tissue effective properties. This interpretation is based on tissue constitutive models. We have pursued the further development of the simplest tissue model on the scale of the single axon, consisting of unidirectional composite with axonal fibers embedded in a glial matrix. On the basis the results of a prior 2D study [10], a biphasic 3D REV model was deployed. The consistency of the stress distribution between 2D REV and 3D REV models in the axial plane (parallel to the fiber direction), as well as the agreement with exact result of the transverse moduli, bolsters the validity of the results.

The sensitivity analysis reveals that the effective transverse modulus is higher than, and increases faster than, its effective axial counterpart as the axon/glia moduli ratio increases at *VF*=0.7. We proved our hypothesis that WM is anisotropic in shear, and this anisotropy can be related to the intrinsic mechanical properties (of its constituents) and the microstructure. In the future, the 3D REV model can be utilized as a base unit of large-scale WM models, including additional geometric information in brain tissue, such as the axon tortuosity and axon-axon tethering via myelin.

ACKNOWLEDGEMENTS

Support was provided by NSF Grants CMMI-1436743, CMMI-1437113, CMMI-1762774, CMMI-1763005, and the R.A. Pritzker endowed chair.

REFERENCES

[1] Johnson, C.L., McGarry, M.D.J., Gharibans, A.A., Weaver, J.B., Paulsen, K.D., Wang, H., Olivero, W.C., Sutton, B.P., and Georgiadis, J.G., 2013, "Local mechanical properties of white matter structures in the human brain," NeuroImage, 79, pp. 145–152.

[2] Tzschätzsch, H., Kreft, B., Schrank, F., Bergs, J., Braun, J. and Sack, I., 2018, "In vivo time-harmonic ultrasound elastography of the human brain detects acute cerebral stiffness changes induced by intracranial pressure variations," Scientific reports, 8, pp.17888.

[3] Feng, Y., Okamoto, R. J., Namani, R., Genin, G.M., and Bayly, P.V., 2013, "Measurements of mechanical anisotropy in brain tissue and implications for transversely isotropic material models of white matter," Journal of the mechanical behavior of biomedical materials, 23, pp.117-132.

[4] Anderson, A.T., Van Houten, E.E., McGarry, M.D., Paulsen K.D., Holtrop, J.L., Sutton, B.P., Georgiadis, J.G., and Johnson, C.L., 2016, "Observation of direction-dependent mechanical properties in the human brain with multi-excitation MR elastography," Journal of the mechanical behavior of biomedical materials, 59, pp.538-46.

[5] Budday, S., Ovaert, T.C., Holzapfel, G.A., Steinmann, P., and Kuhl, E., 2019, "Fifty Shades of Brain: A Review on the Mechanical Testing and Modeling of Brain," Tissue Archives of Computational Methods in Engineering, pp.1-44

[6] Schmidt, J.L., Tweten, D.J., Badachhape, A.A., Reitera, A.J., Okamoto, R.J., Garbow, J.R., and Bayly, P.V., 2018 "Measurement of anisotropic mechanical properties in porcine brain white matter ex vivo using magnetic resonance elastography," Journal of the Mechanical Behavior of Biomedical Materials, 79, pp.30-7.

[7] Romano, A., Scheel, M., Hirsch, S., Braun, J., and Sack, I., 2012, "In vivo waveguide elastography of white matter tracts in the human brain," Magnetic Resonance in Medicine 68, pp.1410-22.

[8] Gallo, N.R., Cahoon, S.M., Anderson, A.T., Naughton, N.M., Pelegri, A.A., and Georgiadis, J.G., Proc. Intl. Soc. Mag. Reson. Med. 28, (Virtual Conference, 08-14 August 2020), vol. Series 28) pp. 0164.

[9] Carlsen, R. W. and Daphalapurkar, N.P., 2015, "The importance of structural anisotropy in computational models of traumatic brain injury," Frontiers in Neurology, 6, pp.28.

[10] Sullivan, D.J., Wu, X., Gallo, N.R., Naughton, N.M., Georgiadis, J.G., and Pelegri, A.A., 2021, "Sensitivity analysis of effective transverse shear viscoelastic and diffusional properties of myelinated white matter, Physics in Medicine & Biology, 66, pp.035027.

[11] Wu, X., Georgiadis, J.G., and Pelegri, A.A., 2019, "Brain white matter model of orthotropic viscoelastic properties in frequency domain." In ASME International Mechanical Engineering Congress and Exposition 2019, American Society of Mechanical Engineers, Pittsburg, PA, Nov 11-14, 2019.

[12] Wu, X. and Pelegri, A.A., 2020, "Deep 3D convolution neural network methods for brain white matter hybrid computational simulations," In ASME International Mechanical Engineering Congress and Exposition 2020, American Society of Mechanical Engineers, Virtual Online.

[13] Pan, Y., Shreiber, D.I., and Pelegri, A.A., 2011, "A transition model for finite element simulation of kinematics of central nervous system white matter," IEEE Transactions on Biomedical Engineering, 58(12), pp. 3443-3446.

[14] Pan, Y., Sullivan, D., Shreiber, D.I., and Pelegri, A.A., 2013, "Finite element modeling of CNS white matter kinematics: use of a 3D RVE to determine material properties," Frontiers in Bioengineering and Biotechnology, 1, pp.19.

[15] Singh, S., Pelegri, A.A., and Shreiber, D.I., 2015, "Characterization of the three-dimensional kinematic behavior of axons in central nervous system white matter," J. Biomechanics and Modeling in Mechanobiology,14(6), pp.1303- 1315.

[16] Arbogast, K.B. and Margulies, S.S., 1999, "A fiber-reinforced composite model of the viscoelastic behavior of the brainstem in shear," Journal of Biomechanics, 32, pp. 865-70.

[17] Abolfathi, N., Naik, A., Chafi, M.S., Karami, G., and Ziejewski, M., 2009, "A micromechanical procedure for modelling the anisotropic mechanical properties of brain white matter," Computer Methods in Biomechanics and Biomedical Engineering, 12(3), pp.249-262.

[18] Fornberg, B. and Flyer, N., 2005, "Accuracy of radial basis function interpolation and derivative approximations on 1-D infinite grids," Advances in Computational Mathematics 23(1-2), pp.5-20.

[19] Christensen, R.M. Mechanics of Composite Materials, Dover Publications. (2005).